diversity

MDPI

Article

Microbial Diversity, Selective Isolation and Bioactivity Characterization of Bacterial Populations in Eutrophic Seawater of Coastal East China Sea

Qiao Yang [1,2,*], Bowen Ouyang [3], Bingqian Liu [2] and Xiaoling Zhang [2,*]

[1] Donghai Laboratory, Zhoushan 316021, China
[2] ABI Group, Phycosphere Microbiology Laboratory, Zhejiang Ocean University, Zhoushan 316022, China
[3] College of Arts and Sciences, The University of Tokyo, Tokyo 151-0064, Japan
* Correspondence: qiaoyang1979@whu.edu.cn (Q.Y.); zhangxiaoling@zjou.edu.cn (X.Z.)

Abstract

Marine bacteria possess significant potential for numerous applications including environmental remediation, creation of natural products and medicines, agriculture, and various industrial sectors. In this study, the diversity of bacterial populations in the seawater at the nearshore S1 station which is a frequent red-tide occurrence area in the East China Sea, was characterized using 16S rRNA gene amplicon sequencing analysis. The three predominant phyla in the bacterial communities were identified as Proteobacteria, Actinobacteria, and Bacteroidetes, with the families *Rhodobacteraceae*, *Mycobacteriaceae*, and *Flavobacteriaceae* as the dominant groups, respectively. The bacterial community composition at the S1 station significantly differed from those of the other five investigated coastal sites, and demonstrated its own unique taxonomic associations with the *Rhodobacteraceae* as the keystone species. Functional prediction through KEGG and MetaCyc analyses revealed the presence of an *L*-tryptophan biosynthesis pathway responsible for indole-3-acetic acid (IAA) production. By using the targeted isolation of cultivable bacterial strains, a novel red-pigmented bacterium, designated S1-TA-50, which produced IAA metabolites, was recovered from the S1 station. It was identified as a potential novel species within the genus *Sulfitobacter* in the family *Rhodobacteraceae*. This bacterium demonstrated notable antibacterial activity against four model pathogenic strains and also acted as a new microalgae growth-promoting bacterium with substantial IAA production after bacterial culture optimization. This study contributes to the accumulation of scientific knowledge regarding the dynamics of marine bacterial ecosystems in nearshore eutrophic environments and facilitates a better understanding of phycosphere bacterial roles in coastal ecosystems, as well as the comprehensive utilization of microbial resources.

Keywords: microbial diversity; eutrophic nearshore seawater; marine bacterial population; IAA-producing bacterium; phycosphere bacteria; algae-bacteria interactions

check for updates

Academic Editors: Cong Sun, Angelina Lo Giudice, Lin Xu and Jianyang Li

Received: 10 August 2025
Revised: 13 October 2025
Accepted: 15 October 2025
Published: 17 October 2025

Citation: Yang, Q.; Ouyang, B.; Liu, B.; Zhang, X. Microbial Diversity, Selective Isolation and Bioactivity Characterization of Bacterial Populations in Eutrophic Seawater of Coastal East China Sea. *Diversity* **2025**, *17*, 727. https://doi.org/10.3390/d17100727

Copyright: © 2025 by the authors. Licensee MDPI, Basel, Switzerland. This article is an open access article distributed under the terms and conditions of the Creative Commons Attribution (CC BY) license (https://creativecommons.org/licenses/by/4.0/).

1. Introduction

Marine microorganisms are vital for maintaining marine ecosystem health [1]. Also, they can decompose organic matter and pollutants, purify the ocean environment and maintaining balance [2], and also produce bioactive substances for various applications in medicine, agriculture and the varied industries such as drug and enzyme development [3,4]. Bacterial spatial patterns in oceans are usually influenced by the latitude, distance from

shore, and environmental gradients like salinity, temperature, and nutrients in the seawaters [5,6]. The nearshore regions are the areas which are most affected by human activities, also thus prone to natural disasters such as harmful algal blooms (HABs) usually initiated by toxic marine dinoflagellates such as *Alexandrium* spp. [7]. Therefore, marine microorganisms living in the nearshore areas usually exhibit unique biological traits due to terrestrial runoff, tidal exchange and human activities [8]. They usually display high biodiversity with fluctuations, fostered by nutrient abundance and environmental changes [9]. Moreover, the dominant populations tend to shift rapidly with different seasons and tides [10,11].

Among various types of aquatic microorganisms, phycosphere microbiota (PM), which thrive in the immediate surroundings of algal cells, represent a specialized microbial community widely distributed in global aquatic ecosystems [12,13]. They encompass intricate and dynamic algae-bacteria relationships including mutualistic symbioses and competitive interactions, and exhibit significant potential across a range of applications [14]. These include contributions to environmental bioremediation, advancements in public health through antimicrobial properties, sustainable resource utilization in aquaculture, and innovations in renewable energy sources such as biofuel production [15]. Therefore, uncovering the fundamental mechanisms that govern these complex interactions is crucial for enhancing of deeper understanding of ecological significance and driving practical solutions in these vital sectors [16].

The low culturability of marine microorganisms including phycosphere microbial consortia, is the main bottleneck hindering comprehensive utilization of abundant microbial resources in nature [17]. Thus, for phycosphere bacteria, expanding the the culturability is crucial for elucidating the underlying interactive mechanisms and also greatly beneficial for advancing the multifunctional applications [18]. Previously, we have characterized various phycosphere microbial consortium associated with HAB-forming dinoflagellates which were sampled from varied red-tide occurring areas in the East China Sea [19–25]. Based on our investigations, the *Rhodobacteraceae* exhibited high metabolic versatility including the ability to perform anoxygenic photosynthesis and interact with micro- and macroalgae in both mutualistic and pathogenic ways [26]. This specific bacterial group was found to be one of the most abundant core bacterial groups in various phycosphere community, and thus offering attracting insights into profound importance during phytoplankton–bacteria interactions and seeking for the multiple applications [27].

The coastal region of the East China Sea (ECS) is one of the most rapidly developing areas in China. Nevertheless, there remains a deficiency in research regarding the diversity and potential value of phycosphere microbial resources in this area [11,28–30]. In this study, high-throughput 16S rRNA gene amplicon sequencing was used to compare the biodiversity of bacterial populations in eutrophic seawater from a station where red tides frequently occur, and from five other sites in the nearshore ECS area. Consequently, following a selective isolation procedure for the isolation of cultivable bacteria, a new red-pigmented bacterium designated as S1-TA-50 was isolated from the seawater at station S1. The new isolate was identified as a potential novel species within the genus *Sulfitobacter* in the family *Rhodobacteraceae*, and it exhibited significant antibacterial bioactivity. Additionally, it was shown to be a novel microalgae growth- promoting bacterium with the production of natural auxin indole-3-acetic acid (IAA), which is crucial and multifunctional in metabolic signaling during algae-bacteria interactions [12].

2. Materials and Methods

2.1. Sampler Collection

Seawater samples of the six investigated station sites (Figure S1) in the nearshore ECS area (<10 m depth) were collected as reported previously [10]. Among the investigated

sites (Table S1), the station S1 (LO1_E group) was the nearest site from the island, and it's a nearshore area where offshore blooms of the red tides often occurred with toxic marine dinoflagellate *Alexandrium* spp. as one most common HAB-causing algal species in this sea area [11,31]. For the sampling procedure, three surface seawater samples with three replicates were collected at each station site. Each sample with 3 L volume was passed through 0.22 μm filter membrane, and the obtained filter membranes were stored at −20 °C for the further experiments. The environmental parameters of the seawater including depth, temperature, conductivity, salinity, oxygen and the fluorescence contents (Table S1), were measured by the on-ship CTD equipment (Model: SBE 911plus, Sea-Bird Scientific, Bellevue, WA, USA).

2.2. 16S rRNA Gene Amplicon Sequencing and Data Analysis

The total genomic DNA from the filter membranes of each sample was extracted using the Fast Bacterial Genomic DNA Extraction Kit (Sangon Biotech Co., Ltd., Shanghai, China) following the manufacturer's protocol. Then, the V3–V4 variable region of the bacterial 16S rRNA gene was amplified using the universal bacterial primer pair 338F/806R [9,11]. Libraries for Illumina sequencing of the 16S rRNA gene were constructed using the TruSeq® DNA PCR-Free Sample Preparation Kit (Illumina, San Diego, CA, USA), followed by sequencing on a NovaSeq 6000 PE250 platform at BioMajor (Shanghai, China).

For data analysis, the QIIME2 script (https://qiime2.org) [32] was utilized. Paired-end reads were joined, subjected to quality filtering, and the resulting ASVs clustered using UCLUST with a stringent 97% similarity threshold. ASV phylotypes were assigned against the QIIME-modified SILVA database (v128) applying default parameters [33].

During overall diversity evaluation, to compare α-diversity, the sequencing depth differences were normalized by rarefying all samples to 95% of the minimum sequence size. Seven key α-diversity indices including the Chao1 and Observed Species indices for richness, the Shannon and Simpson indices for diversity, the Faith's P index for evolutionary diversity, the Pielou's evenness index for evenness, and the Good's coverage index for data coverage, were analyzed and compared. The "qiime diversity alpha" plugin calculated α-diversity indices, while the *R* package "ggplot2" (version 3.5.2) facilitated data visualization [34]. For β-diversity assessment, the PCoA analysis based on Bray-Curtis distance effectively displayed group differences, and was visualized again using the "ggplot2" package [35].

To identify species and functions with the most significant inter-group differences, the Orthogonal Partial Least Squares Discriminant Analysis (OPLS-DA) method was applied [36], and the results were visualized using the ggplot2 package. Based on the relative abundance of key microbial species, a co-occurrence network analysis was conducted by calculating Spearman rank correlation coefficients. Correlations that met the *criteria* ($p < 0.05$ and $|r| > 0.6$) were retained, and the gephi software (https://gephi.org/, accessed on 10 August 2025) was utilized for network visualization [37]. Further data visualization was achieved using "qcorrplot" within the "linkET" package [38].

For functional prediction analysis, the PICRUSt2 software (https://huttenhower.sph.harvard.edu/picrust/, accessed on 10 August 2025) was used to predict sample functional abundance based on gene sequence abundance [38]. Predictions were carried out using databases including both MetaCyc (https://metacyc.org) and KEGG (https://www.kegg.jp, accessed on 10 August 2025). The KEGG Pathway Database classifies metabolic pathways into six major categories. Each category is further subdivided into multiple levels. The second level (K-2) encompasses 45 metabolic pathway sub-functions, the third level (K-3) corresponds to the metabolic pathway map, and the fourth level

provides detailed annotation information for each KO in the metabolic pathway [39]. The MetaCyc database comprises 2722 pathways from over 3000 organisms [40].

2.3. CECS-Based Selective Isolation of Cultivable Bacterial Strains

The selective isolation of cultivable bacterial strains from seawater was conducted using our previously reported procedure, known as the Combinational Enhanced Cultivation Strategy (CECS) [20–23]. In brief, marine broth (MB) or marine agar (MA) media, supplemented with 5.24 g/L HEPES as a buffering agent and 300 mL/L natural seawater, were adjusted to a pH of 7.2 ± 0.1. The composite gels were pretreated with micro-nutrients and added to 12-well microplates at a final concentration of 0.251 g/L. Ten microliters of 1:10 serially diluted samples were then added to triplicate 1-mL microplate wells. The microplates were incubated at 28 ± 1.0 °C for 5–10 days. Subsequently, ten microliters of culture were spread on MA plates and cultured at 28 ± 1.0 °C. The bacterial isolates were subjected to further purification and maintained on MA slant tubes for short-term use or preserved as a 25% (*v*/*v*) glycerol suspension at −80 °C for long-term preservation.

2.4. Molecular Identification of Bacterial Strains

The bacterial genomic DNA of the isolate was extracted using a Fast Bacterial Genomic DNA Extraction Kit (Sangon Biotech Co., Ltd., Shanghai, China) following the manufacturer's instructions. A general bacterial primer pair, 29F/1492R, was used to amplify the bacterial 16S rRNA gene sequence, and the PCR was performed according to a previously described procedure [21–23,41]. The related 16S rRNA gene sequences of PCR species within the genus *Sulfitobacter* and type strains from the family *Rhodobacteraceae* were retrieved from the NCBI database. Identification of phylogenetic neighbors and calculation of the pairwise 16S rRNA gene sequence similarities were accomplished using the EzTaxon-e server (http://eztaxon-e.ezbiocloud.net, accessed on 16 May 2025). Sequence alignments were conducted using CLUSTAL_X [42]. Phylogenetic trees were reconstructed using the maximum-likelihood (ML) algorithm in the MEGA software package, version 7.0 [12–15].

2.5. Culture Optimization of Bacterial Strain

For bacterial culture optimization, 1 mL of a 24-h fresh bacterial culture of the strain was taken and mixed with 24 mL of fresh 2216 medium. Subsequently, a 150 µL mixture was added to the wells of a 96-well microplate containing different carbon sources and cultured with shaking at 60 rpm. Throughout the culture period, bacterial growth was monitored by recording optical changes at OD_{600nm} every four hours. Ten selected carbon sources, including cellobiose, fructose, galactose, glucose, glycerol, lactose, maltose, mannose, sucrose, and trehalose, along with a pH range of 5.0–9.0, were used for the culture optimization measurements [19].

2.6. Bioactivity Measurements

2.6.1. Antibacterial Bioactivity Measurements

The tested bacterial strains were cultured in 50 mL of MB (Difco, Becton Dickinson, Franklin Lakes, NJ, USA) for 7 days at 25 °C. The fermentation broth was centrifuged to obtain the cell precipitate, and the metabolites were extracted using 100% methanol (50 mL) in an ultrasonic device, and repeated three times. The combined extracts were evaporated to dryness and redissolved in a DMSO solution (3 mL). The antimicrobial activity was determined against three bacterial strains: *Staphylococcus aureus* ATCC 12600, *Bacillus subtilis* ATCC 6051, and *Escherichia coli* ATCC 25922, and one yeast, *Candida albicans* ATCC 10231, using standard microplate assays [43]. Minimum inhibitory concentration (MIC) studies were performed according to the standard reference method [44]. All results are expressed as the means ± SD. Statistical significance was analyzed using a *t*-test in SPSS Statistics

(version 17.0) and plotted with Origin (version 8.0) (https://www.originlab.com/). A value of $p < 0.05$ was considered statistically significant.

2.6.2. Evaluation of Microalgae Growth-Promoting Bioactivity

The microalgae growth-promoting (MGP) activity in a co-culture system was evaluated using the model microalgae *Alexandrium catenella* LZT09, following a previously reported method [45]. The effects on algal growth were analyzed by counting the cell numbers with a hemocytometer and using a Corning® Cell Counter (Corning Corp., Shanghai, China). All measurements were conducted at least in triplicate, and the results were presented as means ± standard deviation (SD).

2.6.3. Screening for IAA-Producing Bacterial Strains

Bacterial isolates were screened for indole-3-acetic acid (IAA) production using the HPLC method previously reported [46]. In brief, the bacterial strains were cultured in Erlenmeyer flasks containing 50 mL of MB medium at 28 ± 0.5 °C for 7 days with shaking at 150 rpm. Subsequently, the cell cultures were centrifuged at 10,000 rpm for 20 min at 4 °C. The supernatants were then analyzed directly by HPLC equipment. The IAA concentration was determined based on a standard curve, and all assays were carried out at least in triplicate.

3. Results and Discussions

3.1. Comparison of Diversity of Marine Bacterial Populations

Based on 16S rRNA gene high-throughput sequencing analysis, a total of 4,536,219 denoised sequences were obtained for all investigated samples, with the details shown in Table S2. Compared to the other five station sites investigated in this study, the bacterial populations at station S1 (designated as the LO1_E group) exhibited a markedly distinct profile of the number of taxa at each taxonomic level, significantly exceeding the taxa numbers observed at the other five sites (Figure 1A).

At the phylum level, bacterial populations were predominantly dominated by Firmicutes (63.7% to 96.5%). However, at nearshore station S1, the proteobacteria was found to be the predominant phylum (69.8%), followed by the actinobacteria (14.6%) and the bacteroidetes (9.7%) (Figure S2). Similarly, distinct characteristics were evident at the family level for bacterial populations in the station S1. Three families including the *Rhodobacteraceae* (19.2%), *Mycobacteriaceae* (8.80%) and *Flavobacteriaceae* (6.15%), were identified as the dominant groups (>5%) at station S1 (Figure 1B). Additionally, total of 32 taxonomic group at the family level were also found, accounting for about 1–5% of the total microbial populations (Table S3). Meanwhile, bacterial populations in the other five sites consistently featured three dominant families including the *Lactobacillaceae*, *Streptococcaceae* and *Enterococcaceae* (Figure 1B), accounting for the proportion as high as 62.9–94.8% of the total bacterial populations (Figure S3). However, they accounted for less than 0.05% for the S1 station samples (Table S4). This findings distinctly showed the uniqueness of the microbial population at the S1 station compared with the other five near-shore sites. Similar observations were further verified based on analysis of species diversity at the genus level as shown in Figures S4 and S5.

To assess the α-diversity data of the bacterial communities in seawater samples investigated in this study, seven key indices of the α-diversity, including the Chao1, Observed Species, Shannon, Simpson, Faith's PD, Pielou's evenness and the Goods coverage index, were calculated and compared. As shown in Table S5, it was found that among the six station sites investigated, the α-diversity indices of the microbial populations in the seawater sample at station S1 were either higher or significantly different (all $p < 0.0001$) compared to

those of the other five sites (Figure 2). These findings clearly indicated that the abundance and diversity of bacterial populations at station S1 were apparently higher than those at the other five stations. Therefore, the microbial population at station S1 seemed to provide with promising potential for further deep investigation.

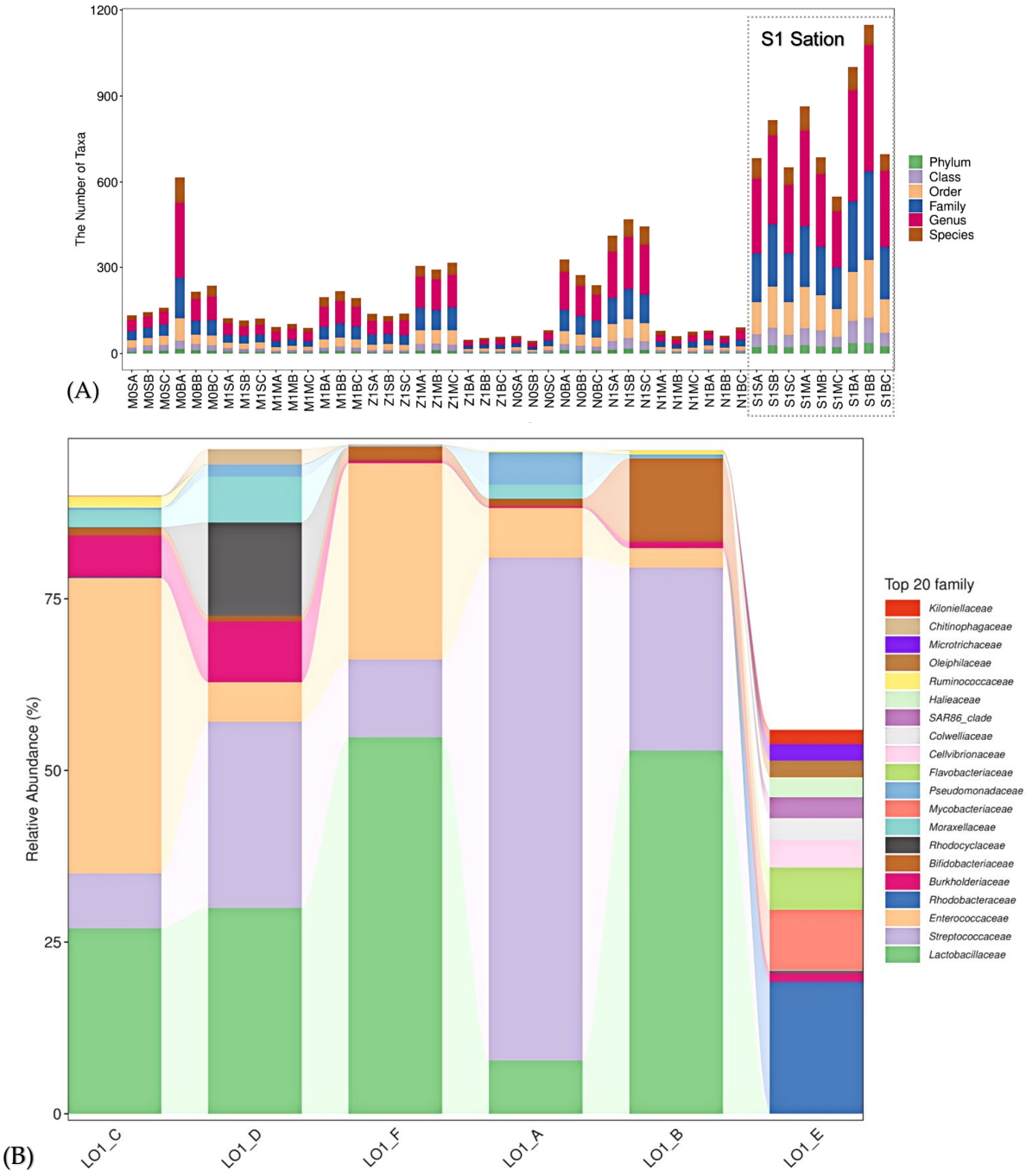


Figure 1. Comparison of bacterial composition of the microbial populations in seawater sample of station S1 (LO1_E) with the other five nearshore sites (labeled as LO1_A, LO1_B, LO1_C, LO1_D, and LO1_F). Pane (**A**): Comparison of the number at all taxa levels of the microbial populations between station S1 (marked with dotted box) and the other five stations. Pane (**B**): Comparison of the relative abundance of top 20 family of the microbial populations. The data of station S1 was highlighted in red box, with the red arrow indicating for family *Rhodobacteraceae* in the S1 station, and the green box for the three dominant families in the other five station samples, respectively.

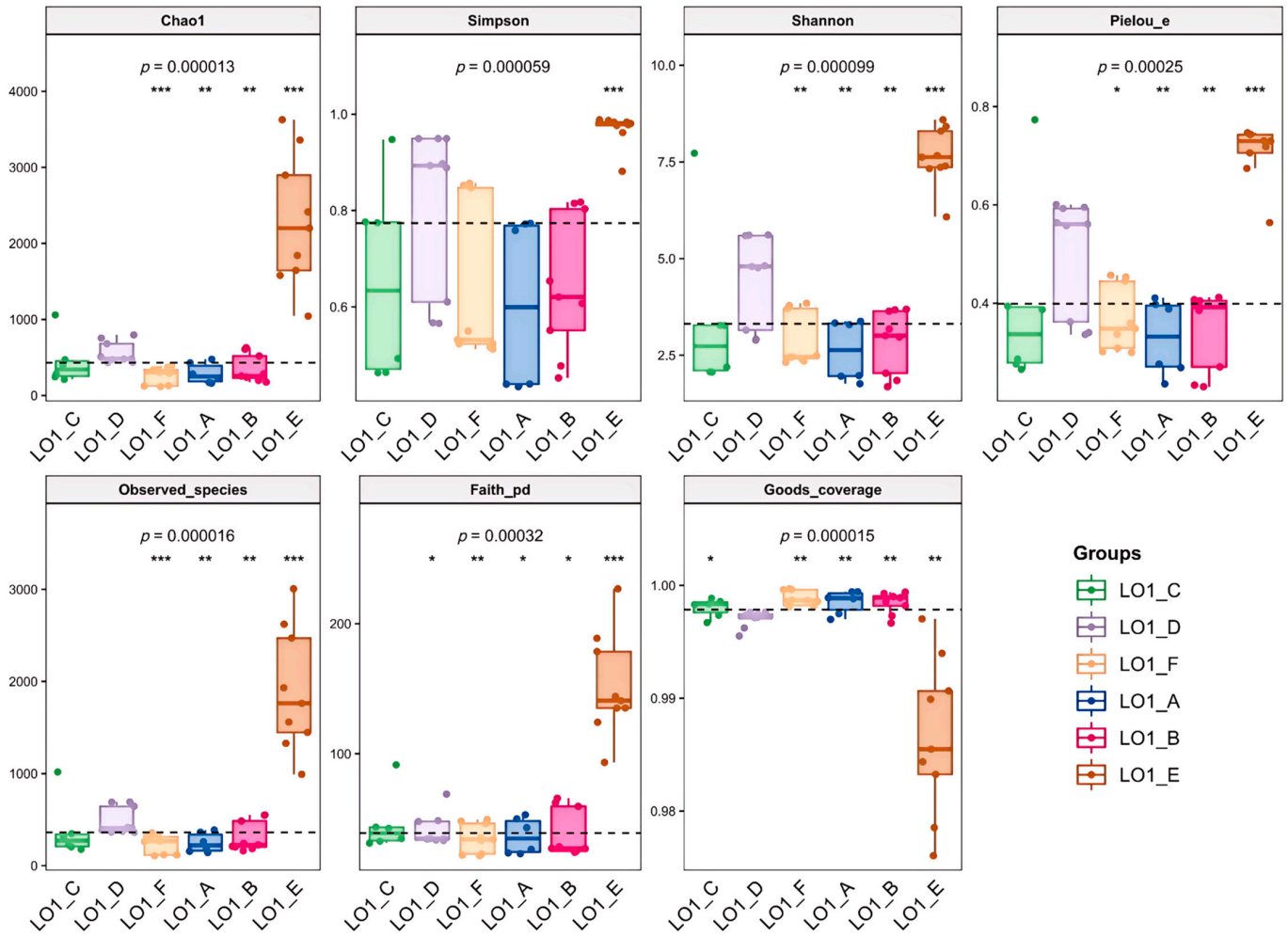


Figure 2. Comparison of the seven indices of the α-diversity for the bacterial populations in the seawater sample of the S1 station (LO1_E group) with the other five nearshore sites (all $p < 0.0001$). The α-diversity index for each station was calculated as the average of all samples, error bars representing SEM. *, $p < 0.05$; **, $p < 0.01$, and ***, $p < 0.001$.

3.2. Functional Prediction of Bacterial Populations

To further explore and reveal whether the functional characteristics of the microbial population in station S1 was alternatively unique compared with other nearshore seawater samples, the biological functions analysis were then predicted based on KEGG pathways and MetaCyc analysis. KEGG annotation (Figure S6) indicated that the parsed Metabolism pathway accounted for about 78.6% of the total was the primary subgroup at the k1-level of KEGG pathway, followed by Genetic Information Processing pathway (accounting for about 10.6%) (Table S5). Additionally, the pathways at the k2-level of KEGG were predominantly composed of the carbohydrate metabolism pathway (10.2%), amino acid metabolism pathway (9.8%), and metabolism of co-factors and vitamins pathway (accounting for about 8.7%) (Figure S6 and Table S6), respectively.

After obtaining abundant data on metabolic pathways, metabolic pathways with significant differences between various groups were then identified. Based on MetaCyc analysis (Table S7), the top five pathways with the highest abundance at the level-2 of the MetaCyc analysis (Figure S7) were identified as nucleoside and nucleotide biosynthesis, amino acid biosynthesis, fatty acid and lipid biosynthesis, co-factor, prosthetic group, electron carrier, and vitamin biosynthesis in the biosynthesis category, and fermentation in the precursors metabolite and energy category, respectively. Additionally,

the predicted TRPSYN-PWY pathway responding for bacterial *L*-tryptophan biosynthesis was obtained based on MetaCyc analysis (Figure 3A). Tryptophan is a precursor for the biosynthesis of IAA, a crucial plant hormone mediating plant-bacteria interactions [12], through a well-established tryptophan- dependent pathway [47,48]. Tryptophan is primarily converted to indole-3-pyruvate (IPA) and then to IAA, or it can be converted to indole-3-acetamide (IAM) and then to IAA [49,50].

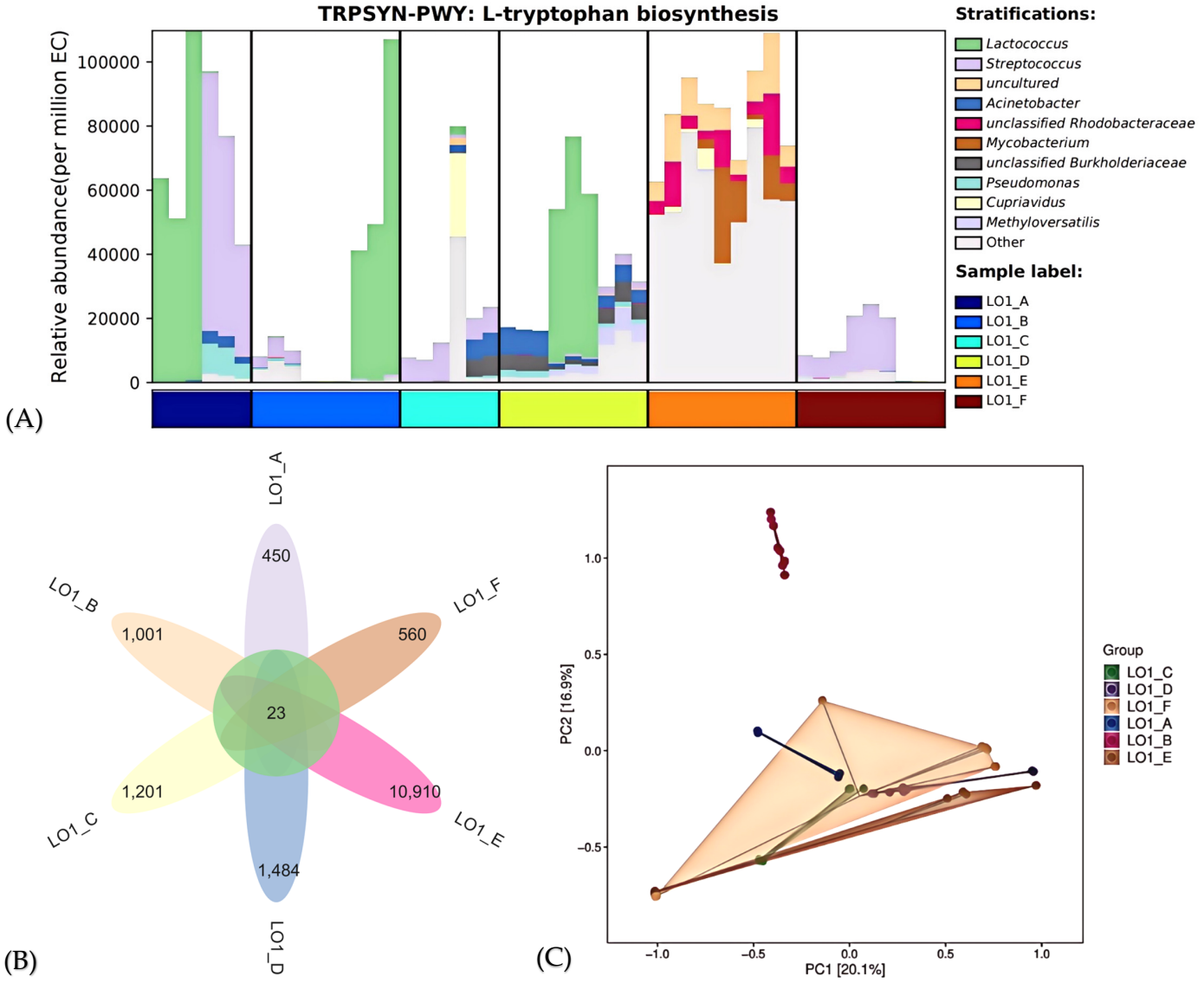


Figure 3. Functional prediction of bacterial populations of station S1 (LO1_E). Pane (**A**): The predicted TRPSYN-PWY pathway responding for bacterial L-tryptophan biosynthesis based on MetaCyc analysis. Pane (**B**): Venn diagram of numbers of the shared and unique bacterial species in microbial populations of six investigated sites. Pane (**C**): The OPLS-DA analysis of bacterial populations based on sample ordination diagram (Pane (**B**)).

To reveal the common and unique species among different groups, a Venn diagram was constructed based on the obtained ASV abundance data. Based on the result shown in Figure 3B, the microbial populations in the six surveyed stations collectively demonstrated a total of 15,629 bacterial species. Remarkably, only 23 species (accounting for 0.14%) were shared across all six stations. In stark contrast, the number of unique species at station S1 (LO1_E group) reached a strikingly high 10,910, accounting for a dominant 99.8% of the total species identified at this station. This finding clearly confirmed the uniqueness of

the microbial population at station S1 during the comparison of diversities among the six investigated sites.

Furthermore, to explore the differences in the spatial populations and functional profiles of the bacterial communities, OPLS-DA analysis was performed to examine bacterial phyla and functions within seawater from all six stations. Based on the obtained significantly different metabolic pathways, species composition of the differential pathways was analyzed using the metabolic pathway abundance data. Based on the results, six core taxa biomarkers at the genus level, including *Mycobacterium*, *Ascidiaceihabitans*, *Lactobacillus*, *Pediococcus*, *Streptococcus*, and *Enterococcus,* were identified. Moreover, these six genus demonstrated significant differences ($p < 0.01$) regarding to their species abundance. Notably, the S1 station distinctly clustered into a separate group compared with the other five stations (Figure 3C).

3.3. Characterization of the Keystone Species in the Microbial Populations in S1 Station

To identify inherent patterns of co-occurrence or co-exclusion in specific microbial communities driven by spatiotemporal changes and environmental processes through association analysis, network analysis is a common method for analyzing microbial communities based on the relationships between microbial members [51]. To analyze the relationships among the bacterial populations at the investigated sites, a co-occurrence network was constructed. It is noteworthy that two independent, unclassified *Rhodobacteraceae* taxonomic units were found in the co-occurrence network for different stations (Figure 4). To further analyze the dominant species in the network, the top 50 nodes in terms of average abundance were extracted based on the abundance data of different species to construct a sub-network for the dominant species. As shown in Figure 4, it was clear that two groups (named Group I and Group II, respectively) emerged in the constructed network (Figure 4). Group I consisted solely of taxa units from the S1 (LO1_E group) station, the first unclassified *Rhodobacteraceae* taxonomic unit demonstrated strong positive correlations with most other taxa units in this group. However, in Group II, six unique taxa units from stations S1 formed a separate subgroup and showed strong positive intra-species associations. This subgroup was found to be centered around an unclassified *Rhodobacteraceae* taxonomic unit, which demonstrated positive associations with all taxonomic units within the species from the S1 station, and negative associations with all taxonomic units outside of the S1 station (Figure 4). This observation confirmed the unique characteristic of the bacterial diversity at the S1 station and demonstrated the *Rhodobacteraceae* as a keystone species for the microbial population at the S1 station. Consequently, the microbial population in the seawater of the S1 station was designated as a target for the selective isolation of culturable bacteria during the following research exploration.

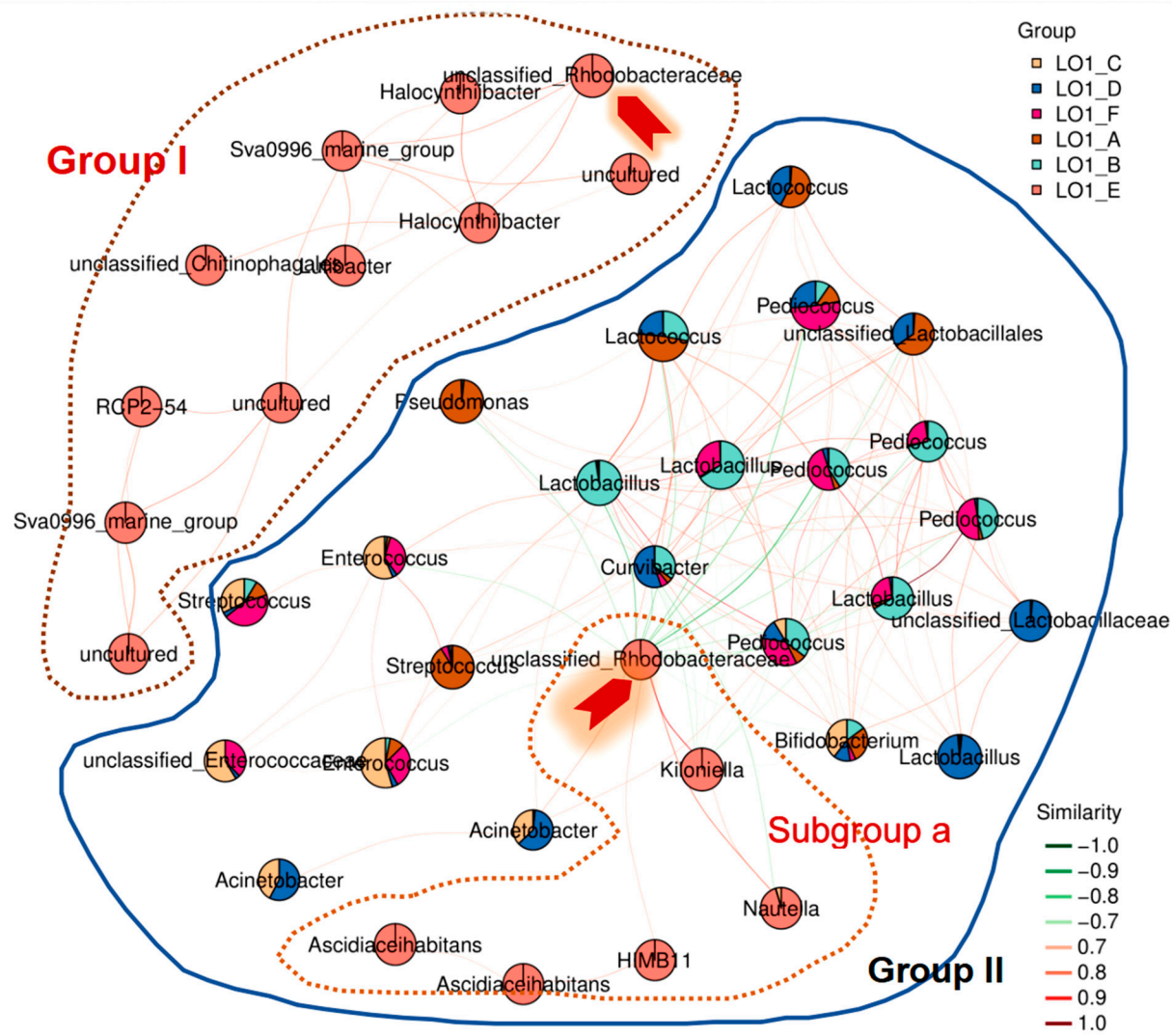


Figure 4. Co-occurrence network analysis of the bacterial populations in investigated six stations. The constructed sub-network diagram with grouped abundance for the dominant species in the network, the top 50 nodes in terms of average abundance based on the abundance data of different species were then extracted to construct the sub-network. Different colors represent various phyla, the size of the nodes represents the size of the abundance, and the lines represent the correlation, with the red indicating positive correlation and green indicating negative correlation. The data only showed correlation relationships whit $p < 0.05$ and $|r| > 0.6$. The two unclassified *Rhodobacteraceae* members were marked with red arrows.

3.4. Phylogenetic Characterization of Cultivable Bacterial Strains of S1 Station

Using our CECS procedure, we successfully isolated a total of 42 bacterial strains from the seawater at station S1. Following isolation, we conducted further investigations to discover potential new species. Phylogenetic analysis of 16S rRNA gene sequences revealed that one isolate, designated as strain S1-TA-50, shared a 16S rRNA gene similarity of 96.35% with the type species *Sulfitobacter porphyrae* SCM-1^T [52]. This value was below the threshold of 98.65% for the identification of novel species [53]. Based on the phylogenetic tree constructed from the 16S rRNA gene of strain S1-TA-50 and closely related type strains within the family *Rhodobacteraceae*, strain S1-TA-50 formed a distinct phylogenetic lineage and clustered with three other strains, S1-TA-3, S1-TA-44, and S1-TA-41, all isolated from station S1 (Figure 5). This suggests that strain S1-TA-50 could be a potential new species within the genus *Sulfitobacter* of the family *Rhodobacteraceae*. Interestingly, among the type strains of the genus *Sulfitobacter*, six bacteria, including *S. porphyrae* [53], *S. algicola* [54],

S. alexandrii [21], *S. pseudonitzschiae* [55], *S. undariae* [56], and *S. pacificus* [57], were all isolated from the phycosphere niche. This may indicate an intrinsic relationship between these *Sulfitobacter* members and the host algae causing the HAB occurrence [58–60].

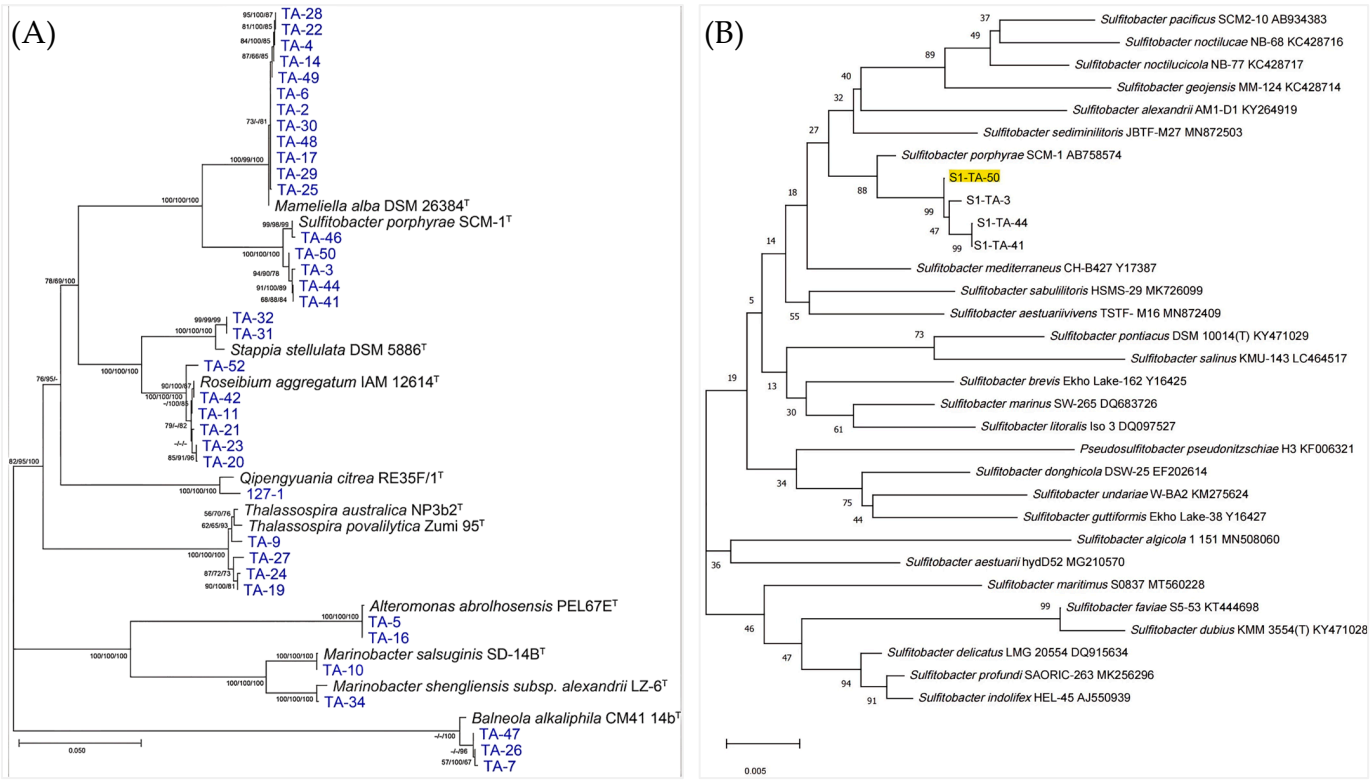


Figure 5. Phylogenetic trees constructed based on 16S rRNA gene sequences of the culturable strains isolated from the S1 station including strain S1-TA-50 (marked in yellow color), with the representative type species in the family *Rhodobacteraceae* (pane **A**), and the type strains in the genus *Sulfitobacter* (pane **B**), respectively.

Strain S1-TA-50 was observed to form lightly red colonies when grown on MA at 28 °C for 2 days. Cells of strain S1-TA-50 were Gram-negative, rod-shaped, and contained polyhydroxyalkanoate (PHA) granules (Figure S8). The strain is motile, aerobic, and weakly positive for anaerobic growth. Transmission Electron Microscopy (TEM) observations showed that the cells of strain S1-TA-50 were approximately 0.3–0.5 μm wide and 1.2–1.8 μm long (Figure S8). Growth occurred at temperatures ranging from 15–37 °C and at pH 5–10, in the presence of 1–4% (*w*/*v*) NaCl.

3.5. Bioactivity Measurement of Isolated Bacterial Strains

Crude extracts were prepared from the bacterial metabolites of four strains (S1-TA-3, S1-TA-41, S1-TA-44, and S1-TA-50) isolated from the S1 station, using standard solvent extraction protocols to isolate bioactive compounds. The antimicrobial activities of these crude extracts were then evaluated against four selected model pathogens: *B. subtilis*, *S. aureus*, *C. albicans*, and *E. coli*. The results obtained from these evaluations, including inhibition zone measurements and relative potency, were compiled and presented in Table 1. Among the tested strains, S1-TA-41, S1-TA-44, and strain S1-TA-50 exhibited varying degrees of inhibitory activity against all four pathogens, with strain S1-TA-50 demonstrating the highest antimicrobial bioactivity, particularly showing strong suppression against three pathogens, *S. aureus*, *E. coli* and *C. albicans*. In contrast, the extracts isolated from strain S1-TA-3 consistently demonstrated no discernible inhibitory bioactivity against

any of the four tested pathogens, indicating a lack of bioactive antimicrobial agents in this bacterial isolate.

Table 1. Antimicrobial bioactivity analysis of the four bacterial strains.

Tested Strains	Antibacterial Activity (MIC, μg/mL)			
	B. subtilis	***S. aureus***	***C. albicans***	***E. coli***
S1-TA-3	>100	>100	>100	>100
S1-TA-41	25.4	15.6	12.8	10.7
S1-TA-44	22.1	16.7	10.5	9.8
S1-TA-50	12.3	3.3	5.4	3.6

Notes: MIC, Minimum Inhibitory Concentration; *S. aureus*, *Staphylococcus aureus* ATCC 12600; *B. subtilis*, *Bacillus subtilis* ATCC 6051; *E. coli*, *Escherichia coli* ATCC 25922; *C. albicans*, *Candida albicans* ATCC 10231.

3.6. Culture Optimization of IAA Production by Strain S1-TA-50

Plant-microbe interactions involve bacteria producing the plant hormone indole-3-acetic acid (IAA) to influence plant growth. IAA also functions as a signaling molecule in microbes, regulating gene expression and physiology to facilitate colonization strategies [61,62]. Strain S1-TA-50 was a new microalgae growth-promoting bacterium (Figure S9), and it's also identified as a producer of IAA. Given the vital roles of IAA during plant-microbe interactions, associated bacteria have developed complex mechanisms to manipulate its levels, with phycosphere bacteria synthesizing and excreting IAA to mediate and influence the interactions [12,63,64].

To advance subsequent algae-bacteria interactions research and promote its application, it is very necessary to optimize the IAA yield of the isolated IAA-producing bacterial strain. Initial experiments identified the initial pH and the type of carbon source in the culture medium as the primary factors affecting IAA production in strain S1-TA-50. Consequently, ten alternative carbon sources and a defined pH range were evaluated to further optimize bacterial culture conditions. The pH testing revealed that strain S1-TA-50 exhibited optimal bacterial growth within a pH range of 8.0–9.0. Additionally, the fastest bacterial growth occurred when glucose was the sole carbon source in the medium at pH 9.0 (Figure 6A). However, IAA accumulation profiling in strain S1-TA-50 indicated that the highest IAA yield was achieved at pH 9.0 following a total of 60 h of incubation. Under these optimized conditions, strain S1-TA-50 reached its peak bacterial growth after 60 h (Figure 6B, panel a), yielding the maximum IAA concentration of 51.25 ± 6.47 μg/mL. This peak production utilized glucose (10 g/L) as the carbon source, and was cultured at 28 °C with an initial medium pH of 9.0 (Figure 6B, panel b). These results suggest that increasing the medium pH can significantly enhance both bacterial growth and IAA accumulation in strain S1-TA-50, thus potentially establishing a solid foundation for subsequent large-scale IAA cultivation.

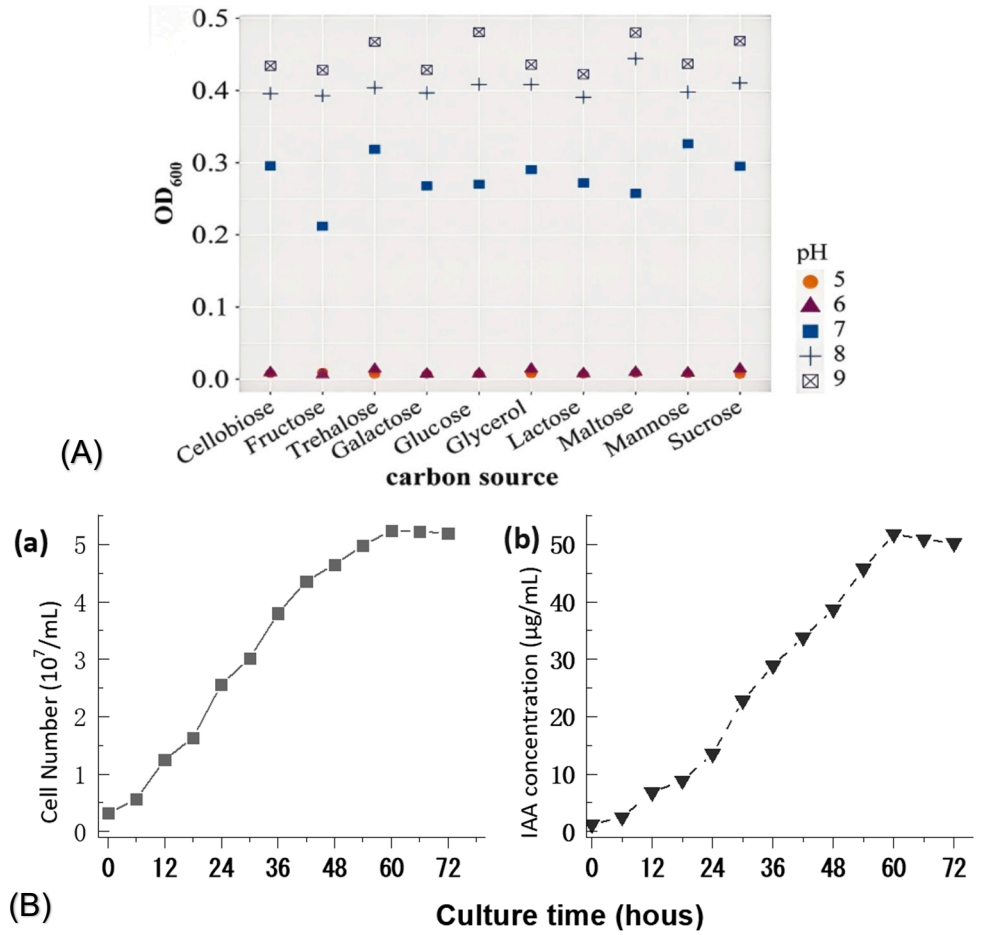


Figure 6. Culture optimization for bacterial growth and IAA production in strain S1-TA-50. Pane (**A**): Effects of the type of carbon sources in the pH range of 5–9 in the culture media on bacterial growth were recorded the optical changes of OD_{600nm} during bacterial culture. Pane (**B**): The accumulation curves of bacterial growth measured by cell number counting (pane **a**), and IAA production (pane **b**) measured by HPLC quantitative analysis under the optimized culture condition.

4. Conclusions

This study utilized 16S rRNA gene amplicon sequencing to reveal the unique distribution pattern of bacterial populations in the eutrophic seawater at the nearshore station S1 in the East China Sea area. Functional prediction through KEGG and MetaCyc analysis indicated that these populations had the *L*-tryptophan biosynthesis pathway, which was associated with indole-3-acetic acid (IAA) production. Selective isolation led to the discovery of a novel cultivable bacterium, designated S1-TA-50, and then was identified as a new species within the genus *Sulfitobacter* in the family *Rhodobacteraceae*. This red-pigmented bacterium demonstrated strong antibacterial activity against four pathogenic strains. Additionally, culture optimization confirmed strain S1-TA-50 as a novel microalgae growth-promoting bacterium with a high capacity for IAA production. This research significantly contributes to our understanding of the dynamics of marine bacterial ecosystems in eutrophic nearshore zones and provides valuable insights into the phycosphere bacterial roles in coastal ecosystems, as well as advancing the comprehensive utilization of these unique microbial resources widely distributed in the nature.

Supplementary Materials: The following supporting information can be downloaded at: https://www.mdpi.com/article/10.3390/d17100727/s1, Table S1: Grouping information and environmental parameters data of the six sampling station sites in this study; Table S2: Statistics of the

sequencing data for each sample in six station sites; Table S3: Statistical table of species taxonomic annotation results; Table S4: Comparison of the abundance of the three dominant families including *Lactobacillaceae*, *Streptococcaceae* and *Enterococcaceae* in six station sites. Table S5: Summary of six indexes data for α-diversity analysis for each samples in six stations; Table S6: KEGG abundance data of the samples; Table S7: MetaCyc abundance data of the samples; Figure S1: Schematic diagram of the sampling station sites in this study. Figure S2: Relative abundance of the top 20 bacterial taxa at the phylum level for each sample of the six station sites; Figure S3: Relative abundance of the top 20 bacterial taxa at the family level for each sample of the six station sites; Figure S4: Relative abundance of the top 20 bacterial taxa at the genus level for each station site; Figure S5: Species taxonomic hierarchy tree with abundance information of bacterial diversity of six stations; Figure S6: Comparison of the relative abundance of KEGG pathways; Figure S7: Comparison of the relative abundance of MetaCyc pathways. Figure S8: Transmission electron micrograph of strain S1-TA-50, with white arrows indicating PHA granules inside of the cells; Figure S9: The microalgae growth-promoting potential of bacterial strain S1-TA-50 on algal LZT09.

Author Contributions: Conceptualization, Q.Y. and X.Z.; methodology, B.O. and B.L.; validation, B.O. and B.L.; formal analysis, B.O.; investigation, B.O. and B.L.; resources, Q.Y. and X.Z.; data curation, B.O. and B.L.; writing—original draft preparation, Q.Y.; writing—review and editing, Q.Y. and X.Z.; project administration, Q.Y.; funding acquisition, Q.Y. and X.Z. All authors have read and agreed to the published version of the manuscript.

Funding: This work was supported by the Science Foundation of Donghai Laboratory (DH-2022KF0218), the Natural Science Foundation of Zhejiang (LY23D060005), and the Project from Municipal Science and Technology Bureau of Zhoushan (2022C41018).

Institutional Review Board Statement: Not applicable.

Informed Consent Statement: Not applicable.

Data Availability Statement: The datasets presented in this study can be found in online repositories. The accession number of the repository of is PRJNA772089.

Acknowledgments: The authors thank the support of the Joint Internship Program in the Yangtze River Estuary and Adjacent Sea Areas for the Undergraduates for seawater sampling assistance.

Conflicts of Interest: The authors declare no conflict of interest.

Abbreviations

The following abbreviations are used in this manuscript:

ABI	Algae-Bacteria Interactions
ASV	Amplicon Sequence Variant
ATCC	American Type Culture Collection
CECS	Combinational Enhanced Cultivation Strategy
CTD	Conductivity, Temperature and Depth
DMSO	Dimethyl Sulfoxide
ECS	East China Sea
HABs	Harmful Algal Blooms
HPLC	High Performance Liquid Chromatograph
KEGG	Kyoto Encyclopedia of Genes and Genomes
MA	Marine Agar
MB	Marine Broth
MGP	Microalgae Growth-Promoting
MIC	Minimum Inhibitory Concentration
IAA	Indole-3-Acetic Acid
OD	Optical Density
OPLS-DA	Orthogonal Partial Least Squares Discriminant Analysis

PCR	Polymerase Chain Reaction
PHA	Polyhydroxyalkanoate
PM	Phycosphere Microbiota
SD	Stand Deviation

References

1. Landry, Z.C.; Vergin, K.; Mannenbach, C.; Block, S.; Yang, Q.; Blainey, P.; Carlson, C.; Giovannoni, S. Optofluidic Single-Cell Genome Amplification of Sub-micron Bacteria in the Ocean Subsurface. *Front. Microbiol.* **2018**, *9*, 1152. [CrossRef]
2. Arrigo, K.R. Marine microorganisms and global nutrient cycles. *Nature* **2005**, *437*, 349–355. [CrossRef]
3. Pietra, F. Secondary metabolites from marine microorganisms: Bacteria, protozoa, algae and fungi. achievements and prospects. *NatProd. Rep.* **1997**, *14*, 453–464. [CrossRef]
4. Sunagawa, S.; Coelho, L.P.; Chaffron, S.; Kultima, J.R.; Labadie, K.; Salazar, G.; Djahanschiri, B.; Zeller, G.; Mende, D.R.; Alberti, A. Structure and function of the global ocean microbiome. *Science* **2015**, *348*, 1261359. [CrossRef]
5. König, G.M.; Kehraus, S.; Seibert, S.F.; Abdel-Lateff, A.; Müller, D. Natural products from marine organisms and their associated microbes. *Chembiochem.* **2006**, *7*, 229–238. [PubMed]
6. Wasserstrom, H.; Kublik, S.; Wasserstrom, R.; Schulz, S.; Schloter, M.; Steinberger, Y. Bacterial populations composition in costal dunes of the Mediterranean along a gradient from the sea shore to the inland. *Sci. Rep.* **2017**, *7*, 40266. [CrossRef] [PubMed]
7. Wang, Z.; Juarez, D.L.; Pan, J.F.; Blinebry, S.K.; Gronniger, J.; Clark, J.S.; Johnson, Z.I.; Hunt, D.E. Microbial communities across nearshore to offshore coastal transects are primarily shaped by distance and temperature. *Environ. Microbiol.* **2019**, *21*, 3862–3872. [CrossRef]
8. Lian, K.; Liu, F.; Li, Y.; Wang, C.; Zhang, C.; McMinn, A.; Wang, M.; Wang, H. Environmental gradients shape microbiome assembly and stability in the East China sea. *Environ. Res.* **2023**, *238*, 117197. [CrossRef]
9. Ouyang, L.; Chen, X.; Zhang, W.; Li, S.; Huang, Q.; Zhang, Y.; Yan, C.; Li, S. High Throughput Sequencing Reveals Distinct bacterial populations and Functional Diversity in Two Typical Coastal Bays. *J. Mar. Sci. Eng.* **2022**, *10*, 1878.
10. Zhang, M.; Jiang, R.; Zhang, J.; Li, K.; Zhang, J.; Shao, L.; He, W.; He, P. The impact of IMTA on the spatial and temporal distribution of the surface planktonic bacteria populations in the surrounding sea area of Xiasanhengshan Island of the East China Sea. *J. Mar. Sci. Eng.* **2023**, *11*, 476. [CrossRef]
11. Wang, Z.; Xie, P.; Dai, J.; Zhang, L.; Yang, Q.; Zhang, X.; Yang, X. Variation in Structure and Functional Diversity of Surface Bacterioplankton populations in the Eastern East China Sea. *J. Mar. Sci. Eng.* **2024**, *12*, 69. [CrossRef]
12. Amin, S.A.; Hmelo, L.R.; van Tol, H.M.; Durham, B.P.; Carlson, L.T.; Heal, K.R.; Morales, R.L.; Berthiaume, C.T.; Parker, M.S.; Djunaedi, B. Interaction and signalling between a cosmopolitan phytoplankton and associated bacteria. *Nature* **2015**, *522*, 98–101. [CrossRef]
13. Zhang, X.L.; Tian, X.Q.; Ma, L.Y.; Feng, B.; Liu, Q.H.; Yuan, L.D. Biodiversity of the symbiotic bacteria associated with toxic marine dinoflagellate *Alexandrium tamarense*. *J. Biosci. Med.* **2015**, *3*, 23–28. [CrossRef]
14. Luo, H.; Moran, M.A. Evolutionary ecology of the marine *Roseobacter* clade. *Microbiol. Mol. Biol. Rev.* **2014**, *78*, 573–587. [CrossRef] [PubMed]
15. Steichen, S.A.; Gao, S.; Waller, P.; Brown, J.K. Association between algal productivity and phycosphere composition in an outdoor *Chlorella sorokiniana* reactor based on multiple longitudinal analyses. *Microb. Biotechnol.* **2020**, *13*, 1546–1561. [CrossRef]
16. Yan, Z.; Chen, B.; Yang, Y.; Yi, X.; Wei, M.; Ecklu-Mensah, G.; Buschmann, M.M.; Liu, H.; Gao, J.; Liang, W.; et al. Multi-omics analyses of airway host-microbe interactions in chronic obstructive pulmonary disease identify potential therapeutic interventions. *Nat. Microbiol.* **2022**, *7*, 1361–1375. [CrossRef]
17. Lewis, W.H.; Tahon, G.; Geesink, P.; Sousa, D.Z.; Ettema, T.J.G. Innovations to culturing the uncultured microbial majority. *Nat. Rev. Microbiol.* **2021**, *19*, 225–240. [CrossRef]
18. Rappé, M.S.; Connon, S.A.; Vergin, K.L.; Giovannoni, S.J. Cultivation of the ubiquitous SAR11 marine bacterioplankton clade. *Nature* **2002**, *418*, 630–633. [CrossRef]
19. Zhang, X.; Xu, J.; Dai, J.; Zhang, L.; Feng, L.; Tian, X.; Yang, Q. Taxonomic, Phylogenomic and Bioactivity Profiling of Novel Phycosphere Bacterium from Model Cyanobacterium *Synechococcus elongatus* PCC7942. *Marine Drugs* **2024**, *22*, 36. [CrossRef]
20. Zhang, X.L.; Pan, Z.K.; Zhang, J.K.; Liu, B.Q.; Yang, Q. Phycobacteria Biodiversity, Selected Isolation, and Bioactivity Elucidation of New Bacterial Species of Highly Toxic Marine Dinoflagellate *Alexandrium minutum* amtk4. *Microorganisms* **2025**, *13*, 1198. [CrossRef]
21. Yang, Q.; Ge, Y.M.; Iqbal, N.M.; Yang, X.; Zhang, X.L. *Sulfitobacter alexandrii* sp. nov., a new microalgae growth-promoting bacterium with exopolysaccharides bioflocculanting potential isolated from marine phycosphere. *Antonie Van Leeuwenhoek* **2021**, *114*, 1091–1106. [CrossRef] [PubMed]

22. Yang, Q.; Jiang, Z.; Zhou, X.; Zhang, R.; Xie, Z.; Zhang, S.; Wu, Y.; Ge, Y.; Zhang, X. *Haliea alexandrii* sp. nov.; isolated from phycosphere microbiota of the toxin-producing dinoflagellate *Alexandrium catenella*. *Int. J. Syst. Evol. Microbiol.* **2020**, *70*, 1133–1138. [CrossRef] [PubMed]
23. Yang, Q.; Feng, Q.; Zhang, B.P.; Gao, J.J.; Sheng, Z.; Xue, Q.P.; Zhang, X.L. *Marinobacter alexandrii* sp. nov.; a novel yellow-pigmented and algae growth-promoting bacterium isolated from marine phycosphere microbiota. *Antonie Van Leeuwenhoek* **2021**, *114*, 709–718. [CrossRef]
24. Ren, C.Z.; Gao, H.M.; Dai, J.; Zhu, W.Z.; Xu, F.F.; Ye, Y.; Zhang, X.L.; Yang, Q. Taxonomic and Bioactivity Characterizations of *Mameliella alba* Strain LZ-28 Isolated from Highly Toxic Marine Dinoflagellate *Alexandrium catenella* LZT09. *Mar. Drugs* **2022**, *20*, 321. [CrossRef]
25. Zhang, X.L.; Li, G.X.; Ge, Y.M.; Iqbal, N.M.; Yang, X.; Cui, Z.D.; Yang, Q. *Sphingopyxis microcysteis* sp. nov., a novel bioactive exopolysaccharides-bearing *Sphingomonadaceae* isolated from the *Microcystis* phycosphere. *Antonie Van Leeuwenhoek* **2021**, *114*, 845–857. [CrossRef]
26. Isaac, A.; Mohamed, A.R.; Amin, S.A. *Rhodobacteraceae* are key players in microbiome assembly of the diatom Asterionellopsis glacialis. *Appl. Environ. Microbiol.* **2024**, *90*, e0057024. [CrossRef]
27. Roager, L.; Kempen, P.J.; Bentzon-Tilia, M.; Sonnenschein, E.C.; Gram, L. Impact of host species on assembly, composition, and functional profiles of phycosphere microbiomes. *Msystems* **2024**, *9*, e0058324. [CrossRef]
28. Liu, X.; Zang, Y.; Fan, S.; Miao, X.; Fu, M.; Ma, X.; Li, M.; Zhang, X.; Wang, Z.; Xiao, J. Changes in the structure of the microbial community within the phycospheric microenvironment and potential biogeochemical effects induced in the demise stage of green tides caused by *Ulva prolifera*. *Front. Microbiol.* **2024**, *15*, 1507660. [CrossRef]
29. Hu, H.; He, J.; Yan, H.; Hou, D.; Zhang, D.; Liu, L.; Wang, K. Seasonality in spatial turnover of Bacterioplankton along an ecological gradient in the East China Sea: Biogeographic patterns, processes and drivers. *Microorganisms* **2020**, *8*, 1484. [CrossRef] [PubMed]
30. Liu, W.; Bao, Y.; Li, K.; Yang, N.; He, P.; He, C.; Liu, J. The diversity of planktonic bacteria driven by environmental factors in different mariculture areas in the East China Sea. *Mar. Pollut. Bull.* **2024**, *201*, 116136. [CrossRef]
31. Sunagawa, S.; Acinas, S.G.; Bork, P.; Bowler, C.; Tara Oceans Coordinators; Eveillard, D.; Gorsky, G.; Guidi, L.; Iudicone, D.; Karsenti, E.; et al. Tara Oceans: Towards global ocean ecosystems biology. *Nat. Rev. Microbiol.* **2020**, *18*, 428–445. [CrossRef] [PubMed]
32. Hall, M.; Beiko, R.G. 16S rRNA Gene Analysis with QIIME2. *Methods Mol. Biol.* **2018**, *1849*, 113–129.
33. Quast, C.; Pruesse, E.; Yilmaz, P.; Gerken, J.; Schweer, T.; Yarza, P.; Peplies, J.; Glöckner, F.O. The SILVA ribosomal RNA gene database project: Improved data processing and web-based tools. *Nucleic Acids Res.* **2013**, *41*, D590–D596. [CrossRef]
34. Gustavsson, E.K.; Zhang, D.; Reynolds, R.H.; Garcia-Ruiz, S.; Ryten, M. ggtranscript: An *R* package for the visualization and interpretation of transcript isoforms using ggplot2. *Bioinformatics* **2022**, *38*, 3844–3846. [CrossRef]
35. Liu, B.; Liu, Y.; Xu, S.; Wu, Q.; Wu, D.; Zhan, L.; Liao, Y.; Mai, Y.; Zheng, M.; Wang, S.; et al. EasyMultiProfiler: An efficient multi-omics data integration and analysis workflow for microbiome research. *Sci. China Life Sci.* **2025**. [CrossRef]
36. Bylesjö, M.; Rantalainen, M.; Cloarec, O.; Nicholson, J.K.; Holmes, E.; Trygg, J. OPLS discriminant analysis: Combining the strengths of PLS-DA and SIMCA classification. *J. Chemom.* **2006**, *20*, 341–351. [CrossRef]
37. Wickham, H. ggplot2. *Wiley Interdiscip. Rev. Comput. Stat.* **2011**, *3*, 180–185. [CrossRef]
38. Douglas, G.M.; Maffei, V.J.; Zaneveld, J.R.; Yurgel, S.N.; Brown, J.R.; Taylor, C.M.; Huttenhower, C.; Langille, M.G.I. PICRUSt2 for prediction of metagenome functions. *Nat. Biotechnol.* **2020**, *38*, 685–688. [CrossRef] [PubMed]
39. Kanehisa, M.; Furumichi, M.; Sato, Y.; Kawashima, M.; Ishiguro-Watanabe, M. KEGG for taxonomy-based analysis of pathways and genomes. *Nucleic Acids Res.* **2023**, *51*, D587–D592. [PubMed]
40. Caspi, R.; Billington, R.; Keseler, I.M.; Kothari, A.; Krummenacker, M.; Midford, P.E.; Ong, W.K.; Paley, S.; Subhraveti, P.; Karp, P.D. The MetaCyc database of metabolic pathways and enzymes—A 2019 update. *Nucleic Acids Res.* **2020**, *48*, D445–D453. [PubMed]
41. Ge, Y.; Xue, Y.; Yang, Q.; Xing, W.; Zhu, S.; Jiang, W.; Liu, J. Benzalkonium chloride disinfection increases the difficulty of controlling foodborne pathogens identified in aquatic product processing. *J. Hazard. Mater.* **2025**, *488*, 137140. [CrossRef]
42. Dubois, B.; Debode, F.; Hautier, L.; Hulin, J.; Martin, G.S.; Delvaux, A.; Janssen, E.; Mingeot, D. A detailed workflow to develop QIIME2-formatted reference databases for taxonomic analysis of DNA metabarcoding data. *BMC Genom. Data* **2022**, *23*, 53. [CrossRef]
43. Zhu, W.Z.; Wang, S.H.; Gao, H.M.; Ge, Y.M.; Dai, J.; Zhang, X.L.; Yang, Q. Characterization of Bioactivities and Biosynthesis of Angucycline/Angucyclinone Derivatives Derived from *Gephyromycinifex aptenodytis* gen. nov., sp. nov. *Mar. Drugs* **2021**, *20*, 34. [CrossRef]
44. Andrews, J.M. Determination of minimum inhibitory concentrations. *J. Antimicrob. Chemother.* **2001**, *48*, 5–16. [CrossRef] [PubMed]

45. Pathom-Aree, W.; Sattayawat, P.; Inwongwan, S.; Cheirsilp, B.; Liewtrakula, N.; Maneechote, W.; Rangseekaew, P.; Ahmad, F.; Mehmood, M.A.; Gao, F.; et al. Microalgae growth-promoting bacteria for cultivation strategies: Recent updates and progress. *Microbiol. Res.* **2024**, *286*, 127813. [CrossRef] [PubMed]
46. Szkop, M.; Bielawski, W. A simple method for simultaneous RP-HPLC determination of indolic compounds related to bacterial biosynthesis of indole-3-acetic acid. *Antonie Van Leeuwenhoek* **2013**, *103*, 683–691.
47. Zhang, H.; Zhao, W.; Yang, W.; Zhang, H.; Qian, X.; Sun, K.; Yang, Q.; Shen, X.; Zhang, L. Autoinducer-2 enhances defence of *Vibrio furnissii* against oxidative stress and DNA damage by modulation of c-di-GMP signaling via a two-component system. *mBio* **2025**, *16*, e0292224. [CrossRef]
48. Duca, D.R.; Glick, B.R. Indole-3-acetic acid biosynthesis and its regulation in plant-associated bacteria. *Appl. Microbiol. Biotechnol.* **2020**, *104*, 8607–8619. [CrossRef] [PubMed]
49. Pham, T.M.; Bui, X.D.; Trang, L.V.K.; Le, T.M.; Nguyen, M.L.; Trinh, D.M.; Phuong, N.T.D.; Khoo, K.S.; Chew, K.W.; Show, P.L. Isolation of indole-3-acetic acid-producing *Azospirillum brasilense* from Vietnamese wet rice: Co-immobilization of isolate and microalgae as a sustainable biorefinery. *J. Biotechnol.* **2022**, *349*, 12–20. [CrossRef]
50. Duca, D.; Lorv, J.; Patten, C.L.; Rose, D.; Glick, B.R. Indole-3-acetic acid in plant-microbe interactions. *Antonie Van Leeuwenhoek.* **2014**, *106*, 85–125. [CrossRef]
51. Needham, D.M.; Sachdeva, R.; Fuhrman, J.A. Ecological dynamics and co-occurrence among marine phytoplankton, bacteria and myoviruses shows microdiversity matters. *ISME J.* **2017**, *11*, 1614–1629. [CrossRef]
52. Fukui, Y.; Abe, M.; Kobayashi, M.; Shimada, Y.; Saito, H.; Oikawa, H.; Yano, Y.; Satomi, M. *Sulfitobacter porphyrae* sp. nov., isolated from the red alga *Porphyra yezoensis*. *Int. J. Syst. Evol. Microbiol.* **2014**, *64*, 438–443. [CrossRef] [PubMed]
53. Elbir, H. Updating the Relationship Between the Threshold Value of Average Nucleotide Identity and Digital DNA-DNA Hybridization for Reliable Taxonomy of *Corynebacterium*. *Vet. Sci.* **2024**, *11*, 661. [CrossRef] [PubMed]
54. Wang, C.N.; Liu, Y.; Wang, J.; Du, Z.J.; Wang, M.Y. *Sulfitobacter algicola* sp. nov.; isolated from green algae. *Arch. Microbiol.* **2021**, *203*, 2351–2356. [CrossRef]
55. Hong, Z.; Lai, Q.; Luo, Q.; Jiang, S.; Zhu, R.; Liang, J.; Gao, Y. *Sulfitobacter pseudonitzschiae* sp. nov., isolated from the toxic marine diatom *Pseudo-nitzschia multiseries*. *Int. J. Syst. Evol. Microbiol.* **2015**, *65*, 95–100. [CrossRef]
56. Park, S.; Jung, Y.T.; Won, S.M.; Park, J.M.; Yoon, J.H. *Sulfitobacter undariae* sp. nov., isolated from a brown algae reservoir. *Int. J. Syst. Evol. Microbiol.* **2015**, *65*, 1672–1678. [CrossRef] [PubMed]
57. Fukui, Y.; Abe, M.; Kobayashi, M.; Satomi, M. *Sulfitobacter pacificus* sp. nov., isolated from the red alga *Pyropia yezoensis*. *Antonie Van Leeuwenhoek* **2015**, *107*, 1155–1163. [CrossRef]
58. Zhang, F.; Fan, Y.; Zhang, D.; Chen, S.; Bai, X.; Ma, X.; Xie, Z.; Xu, H. Effect and mechanism of the algicidal bacterium *Sulfitobacter porphyrae* ZFX1 on the mitigation of harmful algal blooms caused by *Prorocentrum donghaiense*. *Environ. Pollut.* **2020**, *263*, 114475. [CrossRef] [PubMed]
59. Qu, T.; Hou, C.; Zhao, X.; Zhong, Y.; Guan, C.; Lin, Z.; Tang, X.; Wang, Y. Bacteria associated with Ulva prolifera: A vital role in green tide formation and migration. *Harmful Algae* **2021**, *108*, 102104. [CrossRef]
60. Beiralas, R.; Ozer, N.; Segev, E. Abundant *Sulfitobacter* marine bacteria protect *Emiliania huxleyi* algae from pathogenic bacteria. *ISME Commun.* **2023**, *3*, 100. [CrossRef]
61. Gilbert, N.E.; Kimbrel, J.A.; Samo, T.J.; Siccardi, A.J.; Stuart, R.K.; Mayali, X. A bloom of a single bacterium shapes the microbiome during outdoor diatom cultivation collapse. *MSystems* **2025**, *10*, e0037525. [CrossRef] [PubMed]
62. Li, S.; Liu, Q.; Duan, C.; Li, J.; Sun, H.; Xu, L.; Yang, Q.; Wang, Y.; Shen, X.; Zhang, L. c-di-GMP inhibits the DNA binding activity of H-NS in *Salmonella*. *Nat. Commun.* **2023**, *14*, 7502. [CrossRef]
63. Zarei, M.; Rahbar, M.R.; Negahdaripour, M. Interaction of indole-3-acetic acid with horseradish peroxidase as a potential anticancer agent: From docking to molecular dynamics simulation. *J. Biomol. Struct. Dyn.* **2022**, *40*, 4188–4196. [CrossRef]
64. Cheng, X.; Li, X.; Tong, M.; Tong, M.; Wu, J.; Chan, L.L.; Cai, Z.; Zhou, J. Indole-3-acetic acid as a cross-talking molecule in algal-bacterial interactions and a potential driving force in algal bloom formation. *Front. Microbiol.* **2023**, *4*, 1236925. [CrossRef] [PubMed]

Disclaimer/Publisher's Note: The statements, opinions and data contained in all publications are solely those of the individual author(s) and contributor(s) and not of MDPI and/or the editor(s). MDPI and/or the editor(s) disclaim responsibility for any injury to people or property resulting from any ideas, methods, instructions or products referred to in the content.